Stellar Parameters of Main sequence Turn-off Star Candidates Observed with LAMOST and *Kepler*

Y. Q. Wu[1], M.S.Xiang[2],X.F.Zhang[1],T. D. Li[2],S.L. Bi[1],X.W.Liu[3], Y. Huang[3],J.N. Fu1, K. Liu[1],Z.S.Ge[1], J.H. Zhang[1], K.M. Guo[1]

[1]Department of Astronomy, Beijing Normal University, Beijing 100875, P. R. China
[2]National Astronomical Observatories, Chinese Academy of Sciences, Beijing 100012, P. R. China
[3]Department of Astronomy, Peking University, Beijing 100871, P. R. China

Introduction

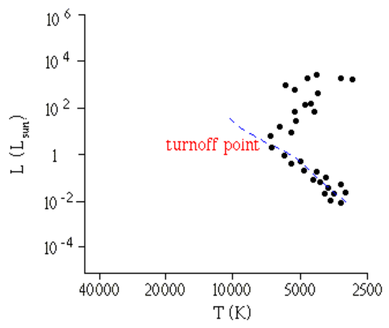

A star begins its evolution as a hydrogen-rich main-sequence star with a hydrogen-burning core. As core hydrogen burning finishes, hydrogen-shell burning starts and the stars expand to large radii, low surface temperatures and high luminosities. The core contracts and heats and the star approaches the sub-giant and red-giant (RGB) branch phase. Main sequence turn-off (MSTO) stars are stars that have reached the point of central hydrogen exhaustion at the end of the MS phase. Because MSTO stars are just leaving the main-sequence to become a sub-giant, their ages are very sensitive to the effective temperature $T_{\rm eff}$, which depend on their masses. Their ages can be relatively determined accurately.

Star clusters are assumed to form from the same gas cloud at the same time, thus, all stars in a cluster have the same age. As well the MSTO stars in clusters are just finishing their main-sequence evolution, and located at the turn points of tips of main-sequence on the Hertzsprung-Russell (HR) diagram, they are easy to be identified. So the ages of MSTO stars in cluster could indicate the age of cluster (e.g. Mackey et al. 2008; Goudfrooij et al. 2009; Yang et al. 2013). Unlike the MSTO stars in clusters, MSTO stars in the field are not easy to be identified from their atmospheric parameters; it is difficult to distinguish them from main sequence or sub-giant stars. To identify filed MSTO stars, precise estimation of atmospheric parameters ($T_{\rm eff}$, log g and [Fe/H]) are required. As the implementation of the LAMOST Experiment for Galactic Understanding and Exploration (LEGUE; Deng et al. 2012; Zhao et al. 2012; Liu et al. 2014) and other spectroscopic surveys such as Sloan Extension for Galactic Understanding and Exploration (SDSS/SEGUE; Yanny et al. 2009), the Radial Velocity Experiment (RAVE; Steinmetz et al. 2006), the Apache Point Observatory Galactic Evolution Experiment (APOGEE; Majewski et al. 2010), stellar atmospheric parameters for millions of stars are delivered from the survey spectra. Typical accuracy of the LAMOST stellar atmospheric parameters reach 100 – 150 K for $T_{\rm eff}$, 0.20 – 0.25 dex for log g and 0.1 – 0.2 dex for [Fe/H] (Xiang et al. 2015b, Wu et al. 2014, Luo et al. 2015, Gao et al. 2015). And hundreds of thousands of MSTO stars have been selected from the LAMOST survey by Xiang et al. (2015a) (hereafter MSTO stars sample) based on stellar atmospheric parameters yielded by the LAMOST Stellar Parameter Pipeline at Peking University (LSP3; Xiang et al. 2015b). The ages of these MSTO stars sample are also estimated, with a claimed uncertainty of about 30 per cent. However, given the low spectral resolving power of LAMOST (R ~1800; e.g. Cui et al. 2012; Deng et al. 2012), accurate stellar parameters, especially surface gravity, are difficult to be determined accurately from the spectra. Therefore, a further sanity examination on the feasibility of method to select MSTO stars sample and obtain accurate fundamental parameters seem to be essential.

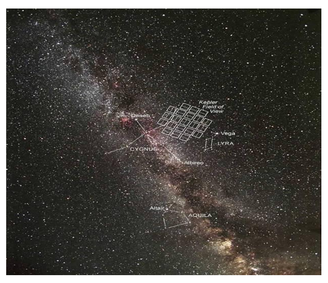

Asteroseismology is a better tool to to derive accurate parameters (Bi et al. 2008; Gilliand et al. 2010; Yang & Meng 2010; Chaplin et al. 2011; Stello et al. 2013; Tian et al. 2015). By asteroseismology, accurate stellar parameters of thousands of stars have been obtained (Chaplin et al. 2014; Huber et al. 2014).It is found that surface gravities yielded by the asteroseismic parameters are much more accurate than the spectroscopic estimates, and reach an accuracy of 0.03 dex (Hekker et al. 2013; Huber et al. 2014). By using asteroseismology, we can identify MSTO stars under the constrains of LAMOST spectral and *Kepler* photometry and determine the stellar parameters especially the age.

In this paper, we determine stellar fundamental parameters of 150 MSTO stars candidates from MSTO stars sample selected with asteroseismic properties. Meanwhile, we compare our results with previous studies by Huber et al. (2014) and Xiang et al. (2015a). In addition, we discuss the impact of uncertainties in $T_{\rm eff}$, log g on the measurement of ages, and reselect these stars as well discuss the contamination rate of these stars.

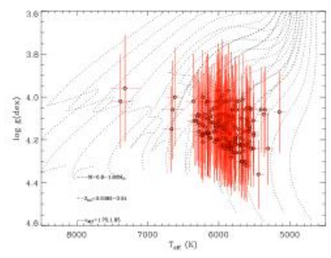

Fig. 1 MSTO stars and evolution tracks in the $T_{\rm eff}$–log g plane. The black dashed lines represent the stellar tracks with masses between 0.8 and 1.8 $M_{\odot}$, $Z_{\rm ini}$ between 0.0085 and 0.04 and $v_{\rm MLT}$ between 1.75 and 1.95. The open circles with error bars represent the 179 MSTO stars with parameters derived by the LSP3, listed in Table 1.

The Sample

The LAMOST-*Kepler* project (De Cat Peter et al. 2015) aims to observe stars in the *Kepler* fields, and determine their atmospheric parameters and radial velocities. The LAMOST (Cui et al. 2012; Zhao et al. 2012) survey has produced a large number of low resolution (R~1800) optical spectra ($\lambda\lambda$3800 – 9000). By September 2014, all the *Kepler* fields had been observed at least once, and 101 086 spectra had beeen collected on 38 LAMOST plates (De Cat Peter et al. 2015). Many of the stars have asteroseismic characteristics deduced from the *Kepler* photometry. These stars have been used to examine and calibrate stellar surface gravities yielded from the LAMOST spectra (Ren et al. 2016; Wang et al. 2016).

The MSTO stars sample are selected from the LAMOST spectra to reserch the structure of the Galactic disk in recent work of Xiang et al. (2015a). They define the MSTO stars using released data of LAMOST DR1 and DR2 constrained with the Yonsei - Yale (YY) isochrones (Demarque et al. 2004) then they obtained 297 042 MSTO stars. In Xiang et al. (2015a), atmospheric parameters were estimated with the LSP3, and the ages of MSTO stars sample were obtained by fitting of interpolating stellar isochrones. These parameters could provide information of Milky Way formation history.

As MSTO stars spending a relatively short timescale in stellar evolution, a relatively small fraction of them expected to be observed, specially which with asteroseismic characteristics. Only 179 MSTO stars candidates with asteroseismic characteristics are selected from the MSTO stars sample. For these stars, atmospheric parameters ($T_{\rm eff}$, [Fe/H] and log g) are estimated by LSP3 pipeline as well asteroseismic characteristics ($\Delta\nu$, $\nu_{\rm max}$) are collected from literature (Hekker et al. 2011; Appourchaux et al. 2012; Mosser et al. 2012; Stello et al. 2013; Huber et al. 2013; Chaplin et al. 2014). These parameters mentioned above are summarized in Table 1.

Table 1: Observational Parameters of 179 targets.

Star KIC	$T_{\rm eff}$ (K)	log g (dex)	[Fe/H] (dex)	$\Delta\nu$ (μHz)	$\nu_{\rm max}$ (μHz)	Ref.
1725815	6195 ± 151	4.08 ± 0.23	0.04 ± 0.11	55.4 ± 1.3	1045 ± 47	(1)
2010607	6113 ± 100	4.09 ± 0.21	0.16 ± 0.09	42.5 ± 1.7	675 ± 86	(1)
2865774	5792 ± 93	4.13 ± 0.20	0.07 ± 0.09	62.7 ± 2.7	1252 ± 90	(1)
2998253	6116 ± 100	4.19 ± 0.19	0.16 ± 0.09	89.0 ± 3.6		(1)
3112152	5967 ± 97	4.10 ± 0.20	-0.03 ± 0.09	63.9 ± 1.9	1219 ± 67	(1)
3123191	6145 ± 101	4.19 ± 0.19	-0.05 ± 0.10	89.8 ± 2.2		(1)
3241581	5577 ± 89	4.21 ± 0.18	0.27 ± 0.09	122.9 ± 1.6		(1)
3344897	6240 ± 104	4.18 ± 0.20	0.07 ± 0.10	46.5 ± 0.8	874 ± 56	(1)
3438633	6082 ± 100	4.12 ± 0.20	-0.17 ± 0.10	55.8 ± 1.7	987 ± 56	(1)
3456181	6236 ± 104	4.17 ± 0.20	0.07 ± 0.10	52.0 ± 0.8	921 ± 30	(1)

Modeling

Input parameters for Grid Calculation.

$[Fe/H]_{\rm ini}$ (dex)	$-0.3 \sim +0.4$	δ[Fe/H] (dex)	0.1
$Z_{\rm ini}$ (dex)	0.0085 – 0.0400		
M ($M_{\odot}$)	$0.8 \sim 2.5$	δM ($M_{\odot}$)	0.02
α	1.75, 1.842, 1.95	$\delta\alpha$	0.1

$$L_{T_{\rm eff}} = \frac{1}{\sqrt{2\pi}\sigma_{T_{\rm eff}}} \exp\left(\frac{-(T_{\rm eff_{obs}} - T_{\rm eff_{model}})^2}{2\sigma^2_{T_{\rm eff}}}\right), \quad (2)$$

$$L_{[Fe/H]} = \frac{1}{\sqrt{2\pi}\sigma_{[Fe/H]}} \exp\left(\frac{-([Fe/H]_{\rm obs} - [Fe/H]_{\rm model})^2}{2\sigma^2_{[Fe/H]}}\right), \quad (3)$$

$$L_{\Delta\nu} = \frac{1}{\sqrt{2\pi}\sigma_{\Delta\nu}} \exp\left(\frac{-(\Delta\nu_{\rm obs} - \Delta\nu_{\rm model})^2}{2\sigma^2_{\Delta\nu}}\right), \quad (4)$$

$$L_{\nu_{\rm max}} = \frac{1}{\sqrt{2\pi}\sigma_{\nu_{\rm max}}} \exp\left(\frac{-(\nu_{\rm max,obs} - \nu_{\rm max,model})^2}{2\sigma^2_{\nu_{\rm max}}}\right). \quad (5)$$

The combined likelihood is

$$L = L_{\Delta\nu}\, L_{\nu_{\rm max}}\, L_{T_{\rm eff}}\, L_{[Fe/H]}. \quad (6)$$

Note that we do not consider the likelihood function for log g because the LSP3 estimates of this quantity may have large systematic errors. We assume that the normalized probability of each model p_i is:

$$p_i = \frac{L_i}{\sum_{i=1}^{N_m} L_i}. \quad (7)$$

Table 3: Fundamental Parameters of 150 stars.

Star KIC	$T_{\rm eff}$ (K)	log g (dex)	[Fe/H] (dex)	M ($M_{\odot}$)	R ($R_{\odot}$)	Age (Gyr)	L ($L_{\odot}$)
MSTO stars							
1725815	6225^{+77}_{-77}	$3.966^{+0.008}_{-0.013}$	$0.01^{+0.10}_{-0.10}$	$1.28^{+0.04}_{-0.04}$	$1.95^{+0.03}_{-0.03}$	$3.94^{+0.55}_{-0.34}$	$5.14^{0.76}_{-0.38}$
2865774	5807^{+72}_{-66}	$4.023^{+0.017}_{-0.013}$	$0.10^{+0.09}_{-0.08}$	$1.12^{+0.04}_{-0.04}$	$1.71^{+0.04}_{-0.04}$	$7.03^{+0.89}_{-0.76}$	$2.99^{0.19}_{-0.16}$
2998253	6107^{+82}_{-76}	$4.214^{+0.018}_{-0.018}$	$0.10^{+0.10}_{-0.11}$	$1.16^{+0.02}_{-0.02}$	$1.39^{+0.03}_{-0.04}$	$5.01^{+0.81}_{-0.61}$	$2.42^{0.17}_{-0.15}$
3112152	5980^{+77}_{-66}	$4.029^{+0.013}_{-0.013}$	$-0.02^{+0.02}_{-0.07}$	$1.14^{+0.04}_{-0.04}$	$1.71^{+0.03}_{-0.03}$	$6.04^{+0.74}_{-0.66}$	$3.37^{0.28}_{-0.20}$
3123191	6134^{+77}_{-66}	$4.217^{+0.012}_{-0.012}$	$-0.02^{+0.03}_{-0.10}$	$1.12^{+0.02}_{-0.04}$	$1.37^{+0.02}_{-0.02}$	$5.16^{+0.61}_{-0.66}$	$2.39^{0.13}_{-0.11}$
3241581	5580^{+77}_{-72}	$4.386^{+0.007}_{-0.008}$	$0.34^{+0.11}_{-0.13}$	$1.02^{+0.04}_{-0.04}$	$1.08^{+0.02}_{-0.03}$	$6.39^{+1.93}_{-1.34}$	$1.02^{0.05}_{-0.06}$
3656476	5543^{+77}_{-66}	$4.224^{+0.004}_{-0.008}$	$0.32^{+0.10}_{-0.10}$	$1.04^{+0.02}_{-0.04}$	$1.31^{+0.01}_{-0.03}$	$9.69^{+1.10}_{-1.59}$	$1.46^{0.09}_{-0.08}$
3967859	5890^{+77}_{-66}	$4.218^{+0.013}_{-0.013}$	$-0.24^{+0.01}_{-0.10}$	$0.94^{+0.04}_{-0.04}$	$1.25^{+0.03}_{-0.03}$	$9.76^{+1.90}_{-1.10}$	$1.70^{0.11}_{-0.11}$
4141376	5898^{+77}_{-72}	$4.404^{+0.008}_{-0.007}$	$-0.29^{+0.11}_{-0.010}$	$0.92^{+0.04}_{-0.02}$	$1.01^{+0.01}_{-0.01}$	$6.66^{+1.71}_{-1.37}$	$1.11^{0.07}_{-0.06}$
4252818	5682^{+77}_{-77}	$4.065^{+0.019}_{-0.019}$	$0.11^{+0.10}_{-0.10}$	$1.06^{+0.02}_{-0.04}$	$1.58^{+0.05}_{-0.05}$	$8.75^{+1.21}_{-0.79}$	$2.35^{0.19}_{-0.17}$
4465324	5776^{+70}_{-72}	$4.188^{+0.012}_{-0.013}$	$0.09^{+0.10}_{-0.10}$	$1.04^{+0.04}_{-0.04}$	$1.36^{+0.03}_{-0.03}$	$8.44^{+1.61}_{-1.19}$	$1.85^{0.14}_{-0.13}$
4543171	5896^{+61}_{-66}	$4.101^{+0.008}_{-0.008}$	$0.20^{+0.10}_{-0.10}$	$1.16^{+0.02}_{-0.04}$	$1.59^{+0.02}_{-0.02}$	$6.05^{+0.91}_{-0.58}$	$2.74^{0.13}_{-0.17}$

Among the 179 MSTO stars candidates, we have obtained stellar parameters of 150 MSTO stars candidates, and found that other 29 stars falling outside of our model grids. For the 29 stars, 25 stars are RGB stars (according to their asteroseismic characteristics) and 4 stars are metal-poor stars with [Fe/H] < −0.3 dex. The stellar parameters of 150 MSTO stars candidates are determined by asteroseismology using maximum likelihood method are listed in Table 3.

Results

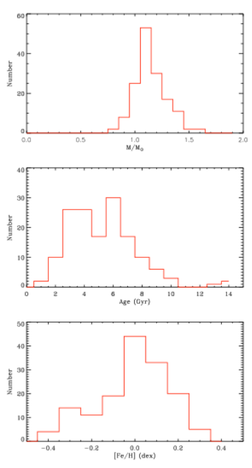

Fig. 2 Distribution of 150 MSTO star with revised parameters. Different parameters lies in different panels, i.e., top: the distribution of masses, middle: the distribution of ages, bottom: distribution of metallicities.

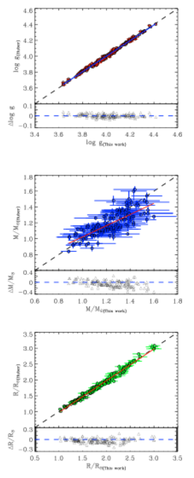

Fig. 3 Comparison of the results of Huber et al. (2014) and our work. Different parameters lies in different panels, i.e., top: gravity log g, middle: mass M, bottom: radius R. The dashed line shows line of equality, solid line shows least square method fitting of both results.

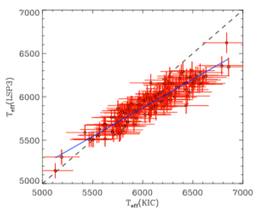

Fig. 4 Comparison the $T_{\rm eff}$ from LAMOST and *Kepler*. The dashed line shows line of equality. Blue solid line shows least squares fitting of temperature.

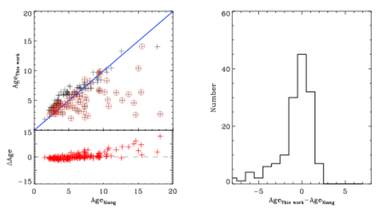

Fig. 5 Comparison the ages from Xiang et al. (2015c). and our work. Left panel: comparison of age calculated by isochrone fitting (Xiang) and asteroseismology (our work). The dashed line shows line of equality and the blue solid line shows least squares fitting of age. The crosses shows the sample of 150 stars and red circles indicate the non-MSTO stars in our work. Right panel: histogram of differences of ages.

Figure 2 illustrates the distribution of mass, age and metallicity for 150 MSTO stars candidates. Their masses are in the range 0.8 – 1.5 $M_{\odot}$ and a peak in the distribution at about 1.1 $M_{\odot}$. The ages are widely distributed in the range 0 – 13 Gyr, with a majority in the range 2 – 8 Gyr. And the metallicities are with the scope of −0.3 – 0.3 dex, with a moderate peak in the distribution near the solar value. Besides, from the Table 3, we find that the typical uncertainties in $T_{\rm eff}$, log g, [Fe/H], M and R are 60 K, 0.009 dex, 0.1 dex, 0.04 $M_{\odot}$ and 0.03 $R_{\odot}$, respectively. The uncertainty in log g is much smaller than that from the LSP3. And the uncertainty in the stellar age varies from 0.4 Gyr for young stars to 1.3 Gyr for old stars, corresponding to a relative error about 9–10 %.

In fact, these 150 MSTO stars candidates are also included in the sample of Huber et al. (2014). Based on the Dartmouth Stellar Evolution Database (DSEP, Dotter et al. 2008), Huber et al. (2014) have derived fundamental parameters by using the asteroseismic quantities and atmospheric parameters in the *Kepler* input catalog (KIC), which mostly are estimated from photometry. But they did not provide important stellar parameter age because the mean [Fe/H] (-0.2 ± 0.3 dex) they used. By comparing the log g, M and R derived by Huber et al. (2014) and our work, we find that our estimation of log g and R are consistent with those of Huber et al., which yield a mean difference of only 0.0002 dex and −0.025 $R_{\odot}$, and a standard deviation of 0.013 dex and 0.056 dex, respectively. However, there is a systematic trend between our mass estimation and those of sample of Huber. Our values are systematically smaller than Huber et al.'s at higher masses. The differences are about 0.1 – 0.2 $M_{\odot}$ for stars around 1.5 $M_{\odot}$. These differences in the stellar masses are mainly caused by differences in the effective temperatures adopted. In Figure 4, we compare $T_{\rm eff}$ derived from the LSP3 and the work of Huber et al. (2014), that exhibits similar trends to those seen in the M panel of Figure 3. As expected, there is a trend that the differences of mass varies with the differences of effective temperatures. Because the $T_{\rm eff}$ derived by the LSP3 are calibrated to the recently deduced metallicity-dependent color–temperature relation of Huang et al. (2015), which is deduced based on stellar interferometry data sets, we believe our results of stellar mass are more reliable than those of the sample of Huber. Beyond that, the stellar metallicity could also affect the determination of stellar mass, but it has only a minor contribution compared with that from the effective temperature.

Furthermore, the results can be used to examine age measurements derived by Xiang et al. (2015a). In Figure 5, we compare the differences between age estimation of this work and those in Xiang et al. (2015a). In the left panel, there is a systematic trend between these two age estimation that our values are systematically younger than the Xiang's. For ages greater than 10 Gyr, the differences are relatively large and cannot be ignored by the study of Galactic structure. The right panel displaces the distribution of the differences among our age estimation and those of Xiang et al. (2015a). The distribution yields a mean difference of 0.53 Gyr (7 %), and a standard deviation of 2.71 Gyr (28 %). The differences in stellar ages are mostly caused by the uncertainty of the LSP3 log g. For instance, KIC 5523099, the LSP3 atmospheric parameters (5513 K, 4.24 dex, 0.03 dex) yield an age of 12.5 Gyr, while our atmospheric parameters (5507 K, 3.79 dex, 0.05 dex) yield 4.6 Gyr, which is 6.9 Gyr younger due to a 0.45 dex overestimate of the LSP3 log g.

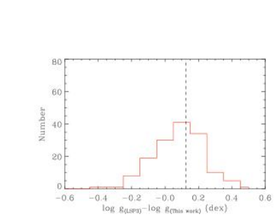

Fig. 7 Distribution of the difference in log g between LSP3 (LSP3) and this work. The dashed line shows the median value of the distribution

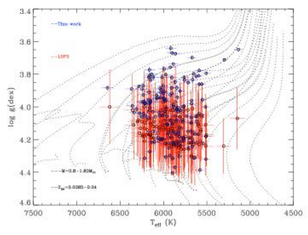

Fig. 8 The location of 150 MSTO candidates with parameters from this work (blue open circles) or the LSP3 (red open circles). Black dashed lines are evolution tracks for M = 0.8–1.5 $M_{\odot}$ and Z = 0.0085–0.04.

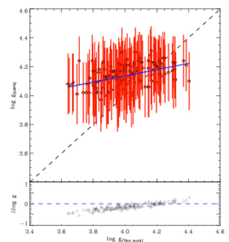

Fig. 6 Comparison of the log g, which derived from LSP3, with our work. The dashed line shows line of equality and the blue solid line shows a least squares fit to log g.

As the uncertainty of the LSP3 log g is the main cause of the differences in stellar ages, we also investigate the impact on different sources of log g. In Figure 6, we perform a comparison of the log g derived from the LSP3 and our work. The figure reveals that log g given by the LSP3 has a linear trend of deviation with our estimated values. The result is consistent with that of Ren et al. (2016), who examined the LSP3 log g with the asteroseismic measurements. To better characterize the bias in the LSP3 log g, we displace a histogram distribution of the differences of log g in Figure 7. The figure exhibits that the LSP3 log g is generally higher than our seismic values by about 0.1 dex, with a calculated standard deviation of 0.16 dex.

Generally, log g derived from asteroseismic parameters is more accurate than that derived from spectroscopy. So we compare the $T_{\rm eff}$ and log g derived from the LSP3 and our work in Figure 8 . The figure indicates that our work yields a sparser distribution, and that a considerable fraction of the stars are located in the sub-giant branch. Through the same method to select MSTO stars in Xiang et al. (2015a), our revised atmospheric parameters indicate that only 79 of the 150 stars are MSTO stars, while the other 71 are either main sequence or sub-giant stars, as indicated in Figure 5. Considering other 29 stars falling outside of our models, we assume 4 metal-poor stars maybe MSTO stars and 25 stars are RGB stars, hence, there are 46 % (83/179) stars of sample are MSTO stars. And about half of the stars indicated to be MSTO by the LSP3 may be main-sequence or sub-giant stars. The contamination rate of the MSTO stars sample may be 54 %. However, a few uncertainties still need to be addressed: the number of stars in our sample is very small, and the definition of MSTO stars is to be considered.

Summary

Under the constrains of atmospheric parameters derived from the LSP3, and seismic characteristics derived from *Kepler* photometry, combined with stellar evolution models we determine the stellar parameters (M, R, Age, L, $T_{\rm eff}$, Z, log g) for 150 MSTO stars candidates. The typical uncertainties for the parameters are 0.04 $M_{\odot}$, 0.03 $L_{\odot}$, 0.03 $R_{\odot}$ for M, L and R, respectively, 0.4 Gyr for young stars and 1.3 Gyr for old stars, as well 60 K, 0.009 dex, 0.1 dex for $T_{\rm eff}$, log g and [Fe/H], separately.

Meanwhile,we compare the log g, radius and mass found in this work with those found by Huber et al. (2014) and find that the log g and radii are consistent, the masses have moderate differences attributable to the different effective temperatures adopted. We also compare the ages found in this work with those found by Xiang et al. (2015a) and find a mean difference of 0.53 Gyr (7 %) and a standard deviation of 2.71 Gyr (28 %). Beyond that, we also reselect these MSTO stars candidates and find that about half of MSTO stars identified with the LSP3 may be main sequence stars or sub-giant stars for which the ages were overestimated. However, the number of stars in our sample is still small, so that our sample may not be representative enough to give a full clarification of contamination rate of the MSTO stars sample. Next work we will construct more comprehensive model grids to include more samples and obtain these stellar parameters.

Acknowlegements

Acknowledgements Guoshoujing Telescope (the Large Sky Area Multi-Object Fiber Spectroscopic Telescope LAMOST) is a National Major Scientific Project built by the Chinese Academy of Sciences. Funding for the project has been provided by the National Development and Reform Commission. LAMOST is operated and managed by the National Astronomical Observatories, Chinese Academy of Sciences.

This work are supported by the grants 10933002 and 11273007 from the National Natural Science Foundation of China, and the Fundamental Research Funds for the Central Universities.